Title	Atmospheric discharge and dispersion of radionuclides during the Fukushima Dai-ichi Nuclear Power Plant accident, 2; Verification of the source term and analysis of regional-scale atmospheric dispersion
Author(s)	Hiroaki Terada, Genki Katata, Masamichi Chino, Haruyasu Nagai
Citation	Journal of Environmental Radioactivity, 112 ; p.141-154
Text Version	Author
URL	http://jolissrch-inter.tokai-sc.jaea.go.jp/search/servlet/search?5034140
DOI	http://dx.doi.org/10.1016/j.jenvrad.2012.05.023
Right	© Elsevier Ltd. All rights reserved. NOTICE: This is the author's version of a work that was accepted for publication in < Journal of Environmental Radioactivity >. Changes resulting from the publishing process, such as peer review, editing, corrections, structural formatting, and other quality control mechanisms, may not be reflected in this document. Changes may have been made to this work since it was submitted for publication. A definitive version was subsequently published in Journal of Environmental Radioactivity, vol. 112, 141-154(October 2012), http://dx.doi.org/10.1016/j.jenvrad.2012.05.023

Atmospheric discharge and dispersion of radionuclides during the Fukushima Dai-ichi Nuclear Power Plant accident. Part II: Verification of the source term and analysis of regional-scale atmospheric dispersion

Hiroaki Terada*, Genki Katata, Masamichi Chino, and Haruyasu Nagai

Japan Atomic Energy Agency

*Corresponding author;

Postal address: 2-4 Shirakata-Shirane, Tokai, Ibaraki, 319-1195 Japan

E-mail: terada.hiroaki@jaea.go.jp

Keywords: Fukushima Dai-ichi Nuclear Power Plant; accident; source term; atmospheric dispersion; surface deposition; WSPEEDI-II; regional-scale

Abstract:

Regional-scale atmospheric dispersion simulations were carried out to verify the source term of

^{131}I and ^{137}Cs estimated in our previous studies, and to analyze the atmospheric dispersion and surface deposition during the Fukushima Dai-ichi Nuclear Power Plant accident. The accuracy of the source term was evaluated by comparing the simulation results with measurements of daily and monthly surface depositions (fallout) over land in eastern Japan from March 12 to April 30, 2011. The source term was refined using observed air concentrations of radionuclides for periods when there were significant discrepancies between the calculated and measured daily surface deposition, and when environmental monitoring data, which had not been used in our previous studies, were now available. The daily surface deposition using the refined source term was predicted mostly to within a factor of 10, and without any apparent bias. Considering the errors in the model prediction, the estimated source term is reasonably accurate during the period when the plume flowed over land in Japan. The analysis of regional-scale atmospheric dispersion and deposition suggests that the present distribution of a large amount of ^{137}Cs deposition in eastern Japan was produced primarily by four events that occurred on March 12, 15 to 16, 20, and 21 to 23. The ratio of wet deposition to the total varied widely depending on the influence by the particular event.

1. Introduction

A large amount of radioactive materials were discharged into the atmosphere during the

Fukushima Dai-ichi Nuclear Power Plant (hereafter referred to as FNPP1) accident in Japan caused by a magnitude 9.0 earthquake and tsunami on March 11, 2011. As a consequence, air dose rates and concentrations of radionuclides in air, soil, drinking water, fresh milk and agricultural crops have increased in areas around and distant from FNPP1 (MAFF, 2011; MEXT, 2011a, 2011b, 2011c, 2011d, 2011e, 2011f; MHLW, 2011).

To understand the atmospheric dispersion processes and assess radiological doses to the public, it is necessary to estimate the source term of the radionuclides during the accident. Thus, efforts to estimate the source term by coupling atmospheric dispersion simulations and environmental monitoring data have been made by several authors (Chino et al., 2011; Katata et al., 2012a, 2012b). The source term of radioactive iodine and cesium from March 12 to April 5 was preliminarily estimated by a reverse estimation method with dust sampling data taken mainly from locations around FNPP1 (Chino et al., 2011). Two major releases of radionuclides on the morning and afternoon of March 15, which contributed to the highest dose rate zones around FNPP1, were estimated by comparing the calculated air dose rates attributed to radionuclides deposited on the ground surface (ground-shine) with the observed ones (Katata et al., 2012a). In part I of this work (Katata et al., 2012b), the release rates of Chino et al. (2011) from the morning of March 12 to late in the night of March 14 were revised by similar methods of using the environmental monitoring

data for air dose rate and air concentrations of radionuclides, which were additionally disclosed by Tokyo Electric Power Company (TEPCO) on May 28 (TEPCO, 2011a) and the Ministry of Economy, Trade and Industry (METI) on June 3 (METI, 2011a) in 2011.

This paper aims to verify the source term of ^{131}I and ^{137}Cs estimated in our previous studies by comparing measured daily and monthly surface depositions of the radionuclides over eastern Japan with those calculated by atmospheric dispersion simulations using the estimated source term. The atmospheric dispersion simulations of ^{131}I and ^{137}Cs from March 12 to May 1 are carried out initially with the source term estimated in our previous articles, (Chino et al., 2011; Katata et al., 2012a, 2012b) (hereafter referred to as the "initial source term"). When there are discrepancies between calculations and measurements of the daily surface depositions of ^{131}I and ^{137}Cs over eastern Japan, and additional environmental monitoring data are available that were not used in estimating the initial source term, the source term is modified to improve predictive accuracy (hereafter referred to as the "refined source term"). On the basis of the simulation results, the processes that resulted in areas with large amounts of ^{137}Cs deposition in eastern Japan during the FNPP1 accident are analyzed.

2. Methods

2.1 Numerical models and simulation conditions

To simulate atmospheric dispersion of radionuclides released from FNPP1 over eastern Japan, the Worldwide Version of System for Prediction of Environmental Emergency Dose Information, WSPEEDI-II (Terada et al., 2008) was used. The simulation system WSPEEDI-II calculates air concentration and surface deposition of radionuclides and radiological doses by successive use of the non-hydrostatic meso-scale meteorological prediction model MM5 (Grell et al., 1994) and the Lagrangian particle dispersion model GEARN (Terada and Chino, 2008). Calculation of dry deposition in GEARN was described in part I of this work (Katata et al., 2012b). The amount of wet deposition of each marker particle was proportional to its radioactivity with a scavenging coefficient Λ (s $^{-1}$) calculated by $\Lambda = \alpha\gamma^{\beta}$. The constants α and β were set to 5.0 × 10^{-5} and 0.8, respectively. Precipitation intensity γ (mm h^{-1}) was calculated by MM5. Wet deposition was considered for particles in atmospheric layers where precipitation (rain, snow, and graupel) or cloud existed. More details of WSPEEDI-II and its prediction performance are described in Terada et al. (2004), Terada and Chino (2005, 2008), and Furuno et al. (2004).

The calculation period in the present study was from 5 Japan Standard Time (JST = UTC + 9 h) on March 12 to 0 JST on May 1. The computational domain includes the eastern area of Japan's main island, Honshu (Fig. 1). The site of FNPP1 is located along the Pacific coast on the eastern

edge of Fukushima Prefecture. To improve the prediction accuracy of meteorological fields, the four-dimensional data assimilation method using meteorological observation data was employed in the model calculations. Wind speed and direction observed at FNPP1, the Fukushima Dai-ni Nuclear Power Plant (hereafter referred to as FNPP2, No.1 in Fig. 1) (METI, 2011b), and surface weather stations were used for data assimilation. The simulation conditions for MM5 and GEARN are summarized in Table 1.

Figure 1

Table 1

2.2 Source term

Dispersion calculations by GEARN were carried out using two sets of source terms, namely, the "initial" and "refined" source terms. The time variation and values of the initial and refined source terms from 5 JST on March 12 to 0 JST on May 1 are shown in Fig. 2 and Table 2, respectively. Regarding the initial source term after 0 JST on April 6, the release rates from 9 JST on April 4 to 0 JST on April 6 estimated by Chino et al. (2011) (No. 28, Table 2) were tentatively extended until 0

JST on May 1 (Fig. 2b). The release heights before 0 JST on March 17 and the dimensions of the volume source, assuming hydrogen explosions at Units 1 and 3 on March 12 and 14, respectively (Nos. 3 and 6, Table 2), were the same as those used in part I of this work (Katata et al., 2012b). The release heights after 0 JST March 17 were set to 20 m by assuming that the location of the leakage was from the primary containment vessel (PCV), although long-range atmospheric dispersion simulations are not very sensitive to the release height.

Firstly, atmospheric dispersion simulations were carried out with the initial source term. Then, the calculated daily surface depositions of ^{131}I and ^{137}Cs were compared with those observed, and the release rates for some periods were refined to reduce discrepancies between calculation and observation. The refined periods were on March 21, 30, and after April 6 when the radioactive plume flowed and deposited mainly over land in Japan, and for which environmental monitoring data were now available, which were disclosed after our previous studies or had not been used previously. Details of this procedure are described in Section 3.2.

Figure 2

Table 2

2.3 Measurement data

Observational data of daily and monthly surface deposition (fallout) and air concentrations of ^{131}I and ^{137}Cs sampled in Japan (MEXT, 2011c) were used for the verification and refinement of the source term. The locations of the sampling points and prefectures where they exist are shown in Fig. 1. The sampling period for daily surface deposition was 24 h starting from 9 JST on each day and the sampling was carried out using bulk samplers. Hereafter, the daily surface deposition on March 18, for example, means the one from 9 JST on March 18 to 9 JST on March 19. All prefectures in the simulation domain have one monitoring point for daily and monthly surface deposition, except for Fukushima and Shizuoka Prefectures, where monthly surface deposition was observed at a different point to the daily one (Fig. 8, shown later). Observations of daily surface deposition started on March 18 at 45 monitoring points except in Fukushima and Miyagi Prefectures (Fig. 1). The measurement was not conducted in Miyagi Prefecture, and it was started later on March 27 at the sampling sites of Fukushima (No. 8, Fig. 1) in Fukushima Prefecture, due to the earthquake damage. The monthly surface deposition measurements in Miyagi Prefecture are also not available for similar reasons. In addition, the map of the surface deposition of ^{137}Cs observed by airborne monitoring (MEXT, 2011d) was used for comparisons of the spatial pattern of cumulative surface

^{137}Cs deposition from calculations with that observed. To refine the initial source term, dust sampling data at FNPP2 (TEPCO, 2011b), Tokai (Furuta et al., 2011), and Setagaya (Tokyo Metropolitan Government, 2011) were used (Nos. 1-3, Fig. 1).

To verify the predictive accuracy of the precipitation calculated by MM5, observational data of daily precipitation from the Japan meteorological agency (JMA), which were the integration of hourly data for 24 h from 9 JST on each day as for the daily surface deposition, were used. For comparison and analysis of the meteorological fields, spatial distributions of rainfall intensity observed by weather radar and surface weather charts from the JMA were also used.

3. Results and Discussion

3.1 Daily surface deposition calculated using the initial source term

Scatter diagrams and statistics of the daily surface deposition of ^{131}I and ^{137}Cs for calculations using the initial source term and for measurements from March 18 to April 30 are shown in Fig. 3a and Table 3, respectively. In Table 3, FA2, FA5, and FA10 denote the percentage of calculations that are within factors of 2, 5, and 10 of the measurements, respectively. To evaluate the accuracy of the initial source term, statistics were calculated for data points for which calculations reproduced observed daily surface depositions greater than 0.1 Bq m^{-2}. The threshold value of 0.1 Bq m^{-2} was

determined from the minimum values of measurements in the simulation area.

Another statistical analysis for agreement between calculations and measurements was carried out based on the method in Bland and Altman (1986). Figure 4 shows so-called "Bland-Altman plots" of the daily surface deposition of ^{131}I and ^{137}Cs for calculations and for measurements from March 18 to April 30. Because there were the tendency that differences between calculations and measurements of the daily surface deposition of ^{131}I and ^{137}Cs increased as the measured ones increased, differences in logarithm of measured and calculated daily surface depositions (subtractions of measurements from calculations) were plotted on the vertical axes. Not averages of two values to be compared, which are usually used in Bland-Altman plots, but measured values themselves were plotted on the horizontal axes for consistency with Fig. 3. Data points for which calculations reproduced observed daily surface depositions greater than 0.1 Bq m^{-2} were plotted the same as Fig. 3. The mean differences in logarithm of measurements and calculations (hereafter referred to as MD) and the standard deviations of the differences (hereafter referred to as SD) are also shown in Fig. 4.

For the daily surface deposition of ^{131}I, a good correlation was found between calculations and measurements, as FA10 was 67.3% and the correlation coefficient was 0.76 (Table 3). In contrast, the correlation of the daily surface deposition of ^{137}Cs was relatively low compared to that of ^{131}I

(the value of FA10 was 54.5% and correlation coefficient was 0.54). For the period after April 6 (crosses in Fig. 3a), the daily surface deposition of ^{137}Cs tends to be underestimated when the calculated values are less than 10 Bq m^{-2} in contrast to those of ^{131}I. In Fig. 4a from the calculation results using the initial source term, although no apparent difference was seen in the SD between ^{131}I and ^{137}Cs, the MD for ^{137}Cs was less than that for ^{131}I. It indicates that the calculated results of ^{137}Cs have larger negative bias in average than those of ^{131}I. Good agreement between calculations and measurements of the daily surface deposition of ^{131}I suggests that the discrepancies in the daily surface deposition of ^{137}Cs are due to errors in the initial source term rather than in the atmospheric dispersion simulation.

Table 3

Figure 3

Figure 4

Some discrepancies between calculations and measurements of the daily surface deposition,

which were expected to be improved by refinement of the initial source term, were found in the Kanto region (Ibaraki, Tochigi, Gunma, Saitama, Chiba, Tokyo, and Kanagawa Prefectures) on March 21, 22, 29, 30, and after April 6. Figure 5 shows a comparison of the daily surface deposition of ^{137}Cs calculated using the initial source term with measurements for the period in which large discrepancies are seen. Daily surface depositions of ^{137}Cs on March 22 (Fig. 5a) were underestimated at the sampling sites of Hitachinaka, Saitama, Ichihara, Shinjuku, and Chigasaki (Nos. 9 and 12-15, Fig. 1). In contrast, daily surface depositions on March 30 were generally overestimated at the sampling sites of Hitachinaka, Utsunomiya, Maebashi, and Saitama (Nos. 9-12, Fig. 1), as shown in Fig. 5b. Furthermore, calculated daily surface depositions of ^{137}Cs were underestimated from April 8 to 11 (not shown in figures). Thus, we modified the initial source term for those periods.

Figure 5

3.2 Refinement of the source term

Source term refinement and its influence on daily surface depositions are described in this section. Figure 3b shows scatter diagrams of daily surface deposition of ^{131}I and ^{137}Cs from calculations

using the refined source term and from measurements. Observed and calculated spatial distributions of daily surface depositions of ^{137}Cs and precipitation are depicted in Figs. 6 and 7, respectively. According to the simulation results, the plume was deposited mainly over land for the periods shown in Fig. 6 (March 12, 14 to 15, 20 to 23, 25, and 30), and over the Pacific Ocean for the other periods in March 2011. Regional-scale atmospheric dispersion and surface deposition of ^{137}Cs during March 2011 are described in Appendix A.

Figure 6

Figure 7

3.2.1 March 21

For the period from 3 to 21 JST on March 21 (No. 16, Table 2), the ^{131}I/^{137}Cs activity ratio was determined from dust sampling data at different points from those used for the release rate of ^{131}I in the initial source term because of the lack of ^{137}Cs measurements. This caused the ^{137}Cs deposition to be underestimated in the Kanto region on March 21 and 22 (Fig. 3a, and Fig. 5a on March 22) by setting a lower release rate of ^{137}Cs, although good agreement was seen for ^{131}I. Considering the

range of observed $^{131}I/^{137}Cs$ activity ratios (from 1.5 to 19.1) in the 12 sampling data at FNPP2, Tokai, and Setagaya (Nos. 1-3, Fig. 1) from 6 to 22 JST on March 21, which were estimated to be influenced by the radioactive plume released from 3 to 21 JST on March 21, and not used previously for the initial source term, we modified the $^{131}I/^{137}Cs$ activity ratio from 131 in the initial source term to 10 (No. 16, Table 2). This means that the release rate of ^{137}Cs over the period is approximately 10 times larger than the initial source term.

The daily surface deposition of ^{137}Cs calculated using the refined source term increased in the Kanto region on March 21 and 22 compared to the calculations using the initial source term. Consequently, by comparing the scatter diagrams and distributions of daily surface deposition (Figs. 3 and 5-6), the calculations using the refined source term show better agreement with the measurements at the sampling sites of Hitachinaka and Utsunomiya (Nos. 9 and 10, Fig. 1) on March 21 (Fig. 6e) and of Hitachinaka, Saitama, Ichihara, Shinjuku, and Chigasaki (Nos. 9 and 12-15, Fig. 1) on March 22 (Fig. 6f).

3.2.2 March 30

The plume flowed to the Kanto region on the morning of March 30, and then changed direction to the northwest of FNPP1 in the afternoon, according to the simulation (see Appendix A). The

release rates including these two periods, the morning and afternoon of March 30, were estimated using only a measurement during the latter period by Chino et al. (2011), and this caused discrepancies in the comparison of daily surface deposition of ^{131}I and ^{137}Cs calculated using the initial source term with the measurements in the Kanto region on March 29 and 30 (Figs. 3a, and Fig. 5a on March 30). Thus, we have added release rates for the morning of March 30, estimated using the dust sampling data at FNPP2 (No. 1, Fig. 1), which were not used by Chino et al. (2011). The release rate of ^{131}I was estimated using the reverse estimation method by dividing measured air concentrations into calculated ones assuming unit release rate (1 Bq h^{-1}) at sampling points (footnote c in Table 2 for the specific values) to be 1.5×10^{13} Bq h^{-1}, and the ^{131}I/^{137}Cs activity ratio were calculated from measured concentrations of ^{131}I and ^{137}Cs to be 1.7. This source term was added between 21 JST on March 29 and 11 JST on March 30 (No. 23, Table 2). The release duration was determined by assuming that each release continued from/to midway between the release times of the sampled air. The release rates of ^{131}I and ^{137}Cs on the morning of March 30 in the refined source term were about one order smaller than those in the initial source term.

In comparison to the calculations using the initial source term, the scatter diagrams and distributions of daily surface deposition calculated using the refined source term show that daily surface depositions of ^{131}I and ^{137}Cs in the Kanto region on March 29 and 30 clearly decreased (Figs.

3, 5, and 6). Daily surface deposition of ^{131}I and ^{137}Cs calculated using the refined source term agreed better with the measurements at the sampling sites of Hitachinaka (No. 9, Fig. 1) on March 29, and of Hitachinaka, Utsunomiya, Maebashi, and Saitama (Nos. 9-12, Fig. 1) on March 30 (Fig. 6i for ^{137}Cs) than those using the initial source term.

3.2.3 After April 6

The value of the ^{131}I/^{137}Cs activity ratio of 4.9 obtained from the dust sampling data from 13:07 to 13:27 JST on April 5 (Chino et al., 2011) was simply assumed to continue until 0 JST on May 1 in the initial source term. This assumption caused an underestimation of the daily surface deposition of ^{137}Cs after April 6, although the calculated ^{131}I deposition showed relatively good agreement (Fig. 3a). In the refined source term, the ^{131}I/^{137}Cs activity ratios after April 6 were calculated from the measured air concentration data and modified to be 2.0 from 17 JST on April 7 to 23 JST on April 13 (No. 29, Table 2), and to be 4.0 from 23 JST on April 13 to 0 JST on May 1 (No. 30, Table 2). These two ^{131}I/^{137}Cs radioactivity ratios were decided on the basis of the mean values from the measured air concentration data sampled at Tokai (No. 2, Fig. 1) from 9 JST on April 8 to 9 JST on April 10, and from 9 JST on April 17 to 9 JST on April 19, respectively, in which the increases of air concentrations during these periods were simulated to be due to the radioactive plumes

discharged from FNPP1 by the model calculation. The release durations were decided by the same method as described in Section 3.2.2. The release rate of ^{137}Cs from 17 JST on April 7 to 23 JST on April 13 particularly increased (Fig. 2b) due to the modification of the source term after April 6.

The above modification of the source term increased the daily surface deposition of ^{137}Cs and improved its predictive accuracy at the sampling sites of Yamagata, Fukushima, Hitachinaka, and Utsunomiya (Nos. 7-10, Fig. 1) on April 8, of Hitachinaka, Utsunomiya, and Ichihara (Nos. 9, 10, and 13, Fig. 1) on April 9, of Fukushima and Utsunomiya (Nos. 8 and 10, Fig. 1) on April 10, and of Hitachinaka, Utsunomiya, Saitama, Ichihara, and Shinjuku (Nos. 9, 10, and 12-14, Fig. 1) on April 11 (not shown in figures).

3.3 Predictive accuracy of calculations with the refined source term

The statistical comparisons of daily surface deposition between measurements and calculations using the initial and refined source terms are summarized in Table 3. For ^{131}I, FA5 and FA10 for the calculations using the refined source term were slightly better than those using the initial source term. Moreover, all statistical values were considerably improved for ^{137}Cs. In comparison to the calculation using the initial source term, FA10 increased from 54.5% to 62.6% and the correlation coefficient from 0.54 to 0.74.

By comparing the Bland-Altman plots between Figs. 4a and b, the MD for ^{137}Cs using the refined source term was closer to zero (identical) than that using the initial source term. The values of SD for both ^{131}I and ^{137}Cs using the refined source term were smaller than those using the initial source term. Because the bands between MD-2SD and MD+2SD in Fig. 4 mean the ranges over which approximately 95% of the differences exist if they are Normally distributed (Gaussian), the above statistics results indicate that there are more calculated values closer to the measurements in the calculation using the refined source term than in the calculation using the initial source term. This also shows that predictive accuracy of the daily surface deposition was enhanced by the source term refinement.

Negative values of MD in Fig. 4b do not indicate that the calculated daily surface depositions were underestimated all over the range of the measured daily surface deposition. It is shown that no apparent biases of under- or over-estimation are seen in the scatter diagrams, except for calculated results with small amounts (less than 10 Bq m^{-2}) of surface deposition (Fig. 3b). The underestimation of these small values is considered to be caused mainly by errors in the meteorological and atmospheric dispersion calculations. Atmospheric dispersion simulations have uncertainties of at least a factor of 5 according to prior studies (e.g., Terada et al., 2004). Considering these errors, it can be concluded that the refined source term is reasonable for the

period when the radionuclides were dispersed and deposited over land in Japan from March 18 to May 1.

Figure 8a and b shows a comparison of calculations using the refined source term and measurements (MEXT, 2011c) of the cumulative surface ^{137}Cs deposition from 5 JST on March 12 to 0 JST on April 1 and from 5 JST on March 12 to 0 JST on May 1. The measurements in Fig. 8b are the summation of monthly surface depositions during March and April in 2011. The calculations agreed well with the measurements at the sampling points in Figs. 8a and b. The result that the distributions of surface deposition of ^{137}Cs with values greater than 1,000 Bq m^{-2} were almost the same in both Figs. 8a and b suggests that the regional-scale surface deposition occurred mainly during March 2011.

The calculated cumulative surface ^{137}Cs deposition from 5 JST on March 12 to 0 JST on May 1 (Fig. 8b) was compared with that from the airborne monitoring (MEXT, 2011d; not shown in figures). It shows that the present regional-scale distribution of ^{137}Cs deposition is characterized by the following areas having amounts of ^{137}Cs deposition exceeding 10,000 Bq m^{-2}:

- Fukushima Prefecture,
- the northeastern coastal area of Miyagi Prefecture,
- the area from the south of Iwate Prefecture to the northwest of Miyagi Prefecture,

- north of Tochigi and Gunma Prefectures,

- north of Ibaraki Prefecture, and

- the area from the south of Ibaraki Prefecture to the northwest of Chiba Prefecture.

The trends of this distribution of surface deposition, observed by airborne monitoring, were roughly reproduced, although some discrepancies were seen between calculations and measurements, e.g., it was underestimated in Tochigi and Gunma Prefectures, and overestimated in the area from the north of the central part of Fukushima Prefecture, via Miyagi Prefecture, to the south of Iwate Prefecture, in particular. These discrepancies are thought to be caused mainly by errors in the meteorological and atmospheric dispersion calculations when the plume encountered precipitation in areas distant from FNPP1 on March 15 (see Appendix A). Considering that the source term on March 15 was verified by the local-scale analysis around FNPP1 (Katata et al., 2012a), these discrepancies are not significant for the verification of the source term. Thus, the source term for the period before March 17, which was not verified by comparison with daily surface deposition, was also validated.

At the end of the simulation period (0 JST on May 1), 37% of the ^{137}Cs discharged into the atmosphere from FNPP1 during the simulation period had been deposited over land in the simulation domain, 21% over ocean in the simulation domain, and the remaining of 42% flowed out of the simulation domain or was still present in the air in the simulation domain. Consequently, less

than half of the total amount of released radionuclides were dispersed and deposited over land in eastern Japan in the results of the calculation. Most of the source term during the period when the plume flowed and deposited over the ocean was not estimated from the dust sampling data, but interpolated from before and after the estimated values, or completely assumed to be the same as in the other period. This can possibly be improved by using global-scale monitoring data (e.g., Masson et al., 2011; Biegalski et al., 2012) in future work.

Figure 8

3.4 Formation processes of large deposition distributions in eastern Japan

According to the analysis of regional-scale atmospheric dispersion and surface deposition of ^{137}Cs from 5 JST on March 12 to 0 JST on May 1 (Figs. 6-8 and Appendix A), it is seen that the distribution of large amounts of ^{137}Cs deposition observed by the airborne monitoring (briefly described in Section 3.3) were produced by the following deposition events:

- dry deposition in the northeastern coastal area of Miyagi Prefecture on March 12 (Fig. 6a),
- wet and dry deposition in Fukushima Prefecture and the north of Tochigi and Gunma Prefectures on March 15 (Fig. 6c),

- dry deposition in the north of Ibaraki Prefecture on March 15 and, possibly, dry and wet deposition on March 16 (Figs. 6b and c),
- wet deposition in the area from the south of Iwate Prefecture to the northwest of Miyagi Prefecture on March 20 (Fig. 6d), and
- wet deposition in the Kanto region, especially in the area from the south of Ibaraki Prefecture to the northwest of Chiba Prefecture, from March 21 to 23 (Figs. 6d-g).

The calculated wet deposition, dry deposition, and the ratio of wet deposition to the total deposition of ^{137}Cs accumulated from 5 JST on March 12 to 0 JST on May 1, are shown in Figs. 9a-c, respectively. A general feature is that the areas corresponding to a large amount of wet deposition were distributed heterogeneously far from FNPP1, as well as around FNPP1 (Fig. 9a), whereas the areas corresponding to a large amount of dry deposition were mainly located near FNPP1 (Fig. 9b). Figure 9c indicates that the ratio of dry deposition to the total was relatively high not only near FNPP1, but also in the northeastern coastal area of Miyagi Prefecture, due to dry deposition on March 12, and in the north of Ibaraki Prefecture, due to dry and wet deposition on March 15 and 16, although the ratio of wet deposition to the total was high in most areas far from FNPP1.

Figure 9

4. Conclusions

The regional-scale atmospheric dispersion and surface deposition of ^{131}I and ^{137}Cs released from the Fukushima Dai-ichi Nuclear Power Plant from 5 JST on March 12 to 0 JST on May 1, 2011 were simulated over eastern Japan using the computer-based nuclear emergency response system, WSPEEDI-II.

In this simulation, the source term, which was estimated in our previous studies primarily using observed air concentrations of radionuclides and air dose rates over land around FNPP1, was verified and refined on the basis of its agreement of calculated daily surface deposition with measurements. Using the refined source term, the calculation reproduced daily and monthly surface deposition distributions over land in eastern Japan, without apparent biases towards under- or over-estimation. Therefore, it is concluded that the source term over the period when the plume flowed over land in Japan is reasonable, although the source term during the period when the plume flowed and deposited over the ocean could not be verified in this study.

The analysis of the regional-scale atmospheric dispersion suggested that the present surface deposition distribution of ^{137}Cs over eastern Japan, observed by airborne monitoring, was produced

mainly by the following events: dry deposition in the northeastern coastal area of Miyagi Prefecture on March 12; wet and dry depositions in Fukushima Prefecture and in the northern part of the Kanto region on March 15 and 16; wet deposition in Iwate and Miyagi Prefectures on March 20; and wet deposition in the Kanto region from March 21 to 23. The ratio of dry deposition to the total was high in places farther away, such as the northeastern coastal area of Miyagi Prefecture and the north of Ibaraki Prefecture, as well as in the areas near FNPP1, although the ratio of wet deposition to the total was high in most areas far from FNPP1.

Appendix A. Daily transport and surface deposition of ^{137}Cs

The atmospheric dispersion and deposition of radionuclides released from FNPP1 were generally reproduced by the simulation with the refined source term (Movie A1). Regional-scale atmospheric dispersion and surface deposition of ^{137}Cs during March 2011 were explained as follows. Detailed analysis of local-scale atmospheric dispersion from March 12 to 17 is described in Katata et al. (2012a, 2012b).

Movie A1

March 12 to 14:

The radioactive plume discharged from FNPP1 first flowed toward the Pacific Ocean over the early morning to the afternoon on March 12. The high-concentration plume around the hydrogen explosion, which occurred at Unit 1 at 15:30 JST on March 12, flowed in the north-northwest direction from FNPP1 and caused a large amount of dry deposition. An increase in air dose rate was observed at the monitoring post of Minami-soma (shown in Fig. 6a) 4.5 h after the explosion (Fukushima Prefecture, 2011). The plume then flowed in the north-northeast direction and produced a large amount of dry deposition in the northeastern coastal area of Miyagi Prefecture (Figs. 6a and 7a). Air dose rates observed at the nuclear power plant in Onagawa (shown in Fig. 6a) were elevated at 0 JST on March 13 when the plume passed through (Tohoku Electric Power, 2011). Afterwards, the plume was transported mainly towards the ocean by the southwesterly wind until the night of March 14.

March 15:

The high-concentration plume started to flow in the south-southwest direction from FNPP1 from late at night on March 14 and caused a large amount of dry deposition along the southeastern coastal area of Fukushima Prefecture and the northeastern area of Ibaraki Prefecture on the morning of March 15 (Figs. 6b and 7b). The plume successively dispersed and caused dry deposition in

Tokyo, Saitama, and Kanagawa Prefectures, although the quantity was smaller than in the above regions. From the afternoon of March 15, precipitation was observed broadly across eastern Japan (Fig. 7c), due to a low pressure system passing through Honshu. The calculated plume encountered the rain band over the areas of Niigata, Gunma, Tochigi, and Fukushima Prefectures, and this caused a large amount of wet deposition in the afternoon (Figs. 6c and 7c). Then, the plume changed its direction clockwise to the northwest of FNPP1, and passed through Miyagi, Yamagata, and Iwate Prefectures during the evening and into the night. In Fukushima Prefecture, the high-concentration plume, due to the major release from FNPP1 in the afternoon, caused significant dry and wet deposition in the area northwest of FNPP1 (Katata et al., 2012a, 2012b).

Although a large amount of surface deposition of ^{137}Cs was observed by airborne monitoring in the north of Tochigi and Gunma Prefectures (MEXT, 2011d), in the calculation, it was mainly seen in the south of Niigata Prefecture and the west of Fukushima Prefecture (Fig. 8b). Because no comparable amount of surface deposition was calculated on other days in the north of Tochigi and Gunma Prefectures, the deposition on March 15 has the largest contribution to the total deposition for the area. From the observed precipitation and air dose rate (MEXT, 2011a; Tochigi Prefecture, 2011), the discrepancy is due to the high-concentration plume passing through Tochigi and Gunma Prefectures before the occurrence of precipitation in the area. In Tochigi Prefecture, additional

surface deposition of ^{137}Cs contained in fog or cloud observed at Okunikko (shown in Fig. 7c) may also contribute to the observed surface deposition.

In the calculation, a significant amount of wet deposition also appeared in the area from the north of the central part of Fukushima Prefecture, via Miyagi Prefecture, to the south of Iwate Prefecture, which was not the case from ground-level and airborne monitoring (MEXT, 2011a, 2011d; Miyagi Prefecture, 2011). Considering that, in the calculation, the principal part of the plume was transported above the clouds (not shown in figures), a possible cause of the discrepancy between calculation and observation is the overestimation of wet deposition in the upper air in the model.

March 16 to 19:

The plume was calculated to have flowed mostly toward the ocean, due to the wind fluctuating from westerly to northwesterly from March 16 to 19. In the observations, however, air dose rate monitoring in the southeast of Fukushima Prefecture and in the east of Ibaraki Prefecture (Fukushima Prefecture, 2011; Ibaraki Prefecture, 2011; KEK, 2011; MEXT, 2011a) during the morning of March 16 suggests that the plume flowed over Ibaraki Prefecture and produced a lot of dry and wet deposition on that morning. The model could not reproduce the above surface deposition because of errors in the calculated wind direction.

March 20:

The plume, which flowed to the east of FNPP1, started to turn clockwise before dawn on March 20. The plume passed over the Kanto region in the morning, and then changed its direction to the northwest of FNPP1 in the afternoon. The plume flowed to the west of Miyagi Prefecture, to the east of Yamagata Prefecture, and to the south of Iwate Prefecture. A large amount of wet deposition was produced in the area, due to precipitation in the evening (Figs. 6d and 7d). The plume started to flow to the south of FNPP1 again late at night.

March 21:

The plume flowed into Ibaraki Prefecture via the ocean on the morning of March 21, then dispersed over the Kanto region and caused a large amount of wet deposition in Ibaraki, Chiba, Saitama, Tokyo, and Kanagawa Prefectures due to precipitation from the morning (Figs. 6e and 7e). Surface depositions were overestimated at the sampling sites of Kofu and Omaezaki (Nos. 17 and 18, Fig. 1) because of the overestimation of daily precipitation.

March 22:

The plume released from FNPP1 on March 22 dispersed mainly in Fukushima and Tochigi Prefectures, and caused wet deposition in the east of Fukushima Prefecture due to precipitation from the night (Figs. 6f and 7f). Meanwhile, the radionuclides released on March 21 remained stagnant in the Kanto region and were deposited by precipitation on March 22.

March 23 to 24:

From the early morning on March 23, the plume was transported along the seaside of Ibaraki and Chiba Prefectures, due to the wind fluctuating from northerly to northwesterly. It flowed into the southeastern part of the Kanto region from the afternoon and produced wet deposition from the evening until late at night (Figs. 6g and 7g). The plume was mostly transported toward the ocean from the morning of March 24 to the morning of March 25.

March 25 to 29:

From the afternoon to the night of March 25, the plume was transported by the southeasterly wind in the northwest direction from FNPP1, and caused wet deposition mainly in Fukushima Prefecture and in the south of Yamagata and Miyagi Prefectures (Figs. 6h and 7h). Then, the plume changed its direction anti-clockwise from northwest to southeast on the morning of March 26. The plume continuously flowed toward the ocean from the morning of March 26 to March 29.

March 30 to 31:

The plume turned clockwise from the east to the southwest of FNPP1 and flowed into the Kanto region on the morning of March 30, and caused wet deposition mainly in Tochigi and Ibaraki Prefectures during the afternoon (Figs. 6i and 7i). The plume from FNPP1 then flowed in the northwest direction from FNPP1 from the afternoon until the night. On March 31, the plume mainly

flowed toward the ocean.

Acknowledgments

The authors wish to express their gratitude to Drs. H. Nakayama, J. Koarashi, M. Ota, A. Furuno, and C. Nakanishi of the Japan Atomic Energy Agency (JAEA) for their contributions to our analysis and preparation of measurement data. We are also indebted to Mr. T. Kakefuda and the Center for Computational Science and e-Systems (CCSE) in JAEA for their support and for providing supercomputer resources in JAEA. We used GPV, surface meteorological observation, surface weather charts, and precipitation radar data from the JMA. We are grateful for their provision of these valuable data.

References

Biegalski, S.R., Bowyer, T.W., Eslinger, P.W., Friese, J.A., Greenwood, L.R., Haas, D.A., Hayes, J.C., Hoffman, I., Keillor, M., Miley, H.S., Moring, M., 2012. Analysis of data from sensitive U.S. monitoring stations for the Fukushima Daiichi nuclear reactor accident. J. Environ. Radioact., in press (doi:10.1016/j.jenvrad.2011.11.007).

Bland, J. M. and Altman, D. G., 1986. Statistical methods for assessing agreement between two methods of clinical measurement. Lancet 1, 307-310.

Chino, M., Nakayama, H., Nagai, H., Terada, H., Katata, G., Yamazawa, H., 2011. Preliminary estimation of release amounts of ^{131}I and ^{137}Cs accidentally discharged from the Fukushima Daiichi nuclear power plant into atmosphere. J. Nucl. Sci. Technol. 48, 1129-1134.

Fukushima Prefecture, 2011. http://www.pref.fukushima.jp/j/7houbu0311-0331.pdf (in Japanese, accessed on December 2, 2011).

Furuno, A., Terada, H., Chino, M., Yamazawa, H., 2004. Experimental verification for real-time environmental emergency response system: WSPEEDI by European tracer experiment. Atmos. Environ. 38, 6989-6998.

Furuta, S., Sumiya, S., Watanabe, H., Nakano, M., Imaizumi, K., Takeyasu, M., Nakada, A., Fujita, H., Mizutani, T., Morisawa, M., Kokubun, Y., Kono, T., Nagaoka, M., Yokoyama, H., Hokama, T., Isozaki, T. Nemoto, M., Hiyama, Y., Onuma, T., Kato, C., Kurachi T., 2011. Results of the

Environmental Radiation Monitoring Following the Accident at the Fukushima Daiichi Nuclear Power Plant. JAEA-Review 2011-035, Japan Atomic Energy Agency (in Japanese with English abstract, available online).

Grell, G.A., Dudhia, J., Stauffer, D.R., 1994. A description of the fifth-generation Penn State/NCAR Mesoscale Model (MM5). NCAR Tech. Note NCAR/TN-398STR, 122 pp.

Ibaraki Prefecture, 2011. http://www.pref.ibaraki.jp/20110311eq/radiation.html (in Japanese, accessed on December 2, 2011).

Katata, G., Terada, H., Nagai, H., Chino, M., 2012a. Numerical reconstruction of high dose rate zones due to the Fukushima Dai-ichi Nuclear Power Plant accident. J. Environ. Radioact., in press (doi:10.1016/j.jenvrad.2011.09.011).

Katata, G., Ota, M., Terada, H., Chino, M., Nagai, H., 2012b. Atmospheric discharge and dispersion of radionuclides during the Fukushima Dai-ichi Nuclear Power Plant accident. Part I: Source term estimation and local-scale atmospheric dispersion in early phase of the accident. J. Environ.

Radioact. 109, 103-113.

KEK (High Energy Accelerator Research Organization), 2011.

http://rcwww.kek.jp/norm/index-e.html (accessed on December 2, 2011).

MAFF (Ministry of Agriculture, Forestry and Fisheries), 2011.

http://www.s.affrc.go.jp/docs/press/110830.htm (in Japanese, accessed on May 4, 2012).

Masson, O., Baeza, A., Bieringer, J., Brudecki, K., Bucci, S., Cappai, M., Carvalho, F.P., Connan, O., Cosma, C., Dalheimer, A., Didier, D., Depuydt, G., De Geer, L.E., De Vismes, A., Gini, L., Groppi, F., Gudnason, K., Gurriaran, R., Hainz, D., Halldorsson, O., Hammond, D., Hanley, O., Holey, K., Homoki, Zs., Ioannidou, A., Isajenko, K., Jankovic, M., Katzlberger, C., Kettunen, M., Kierepko, R., Kontro, R., Kwakman, P.J.M., Lecomte, M., Leon Vintro, L., Leppänen, A.-P., Lind, B., Lujaniene, G., Mc Ginnity, P., Mc Mahon, C., Mala, H., Manenti, S., Manolopoulou, M., Mattila, A., Mauring, A., Mietelski, J.W., Møller, B., Nielsen, S.P., Nikolic, J., Overwater, R.M.W., P álsson, S.E., Papastefanou, C., Penev, I., Pham, M.K., Povinec, P.P., Ramebäck, H., Reis, M.C., Ringer, W., Rodriguez, A., Rulík, P., Saey, P.R.J., Samsonov, V., Schlosser, C., Sgorbati, G., Silobritiene, B.V.,

Söderström, C., Sogni, R., Solier, L., Sonck, M., Steinhauser, G., Steinkopff, T., Steinmann, P., Stoulos, S., Sýkora, I., Todorovic, D., Tooloutalaie, N., Tositti, L., Tschiersch, J., Ugron, A., Vagena, E., Vargas, A., Wershofen, H., Zhukova, O., 2011. Tracking of Airborne Radionuclides from the Damaged Fukushima Dai-Ichi Nuclear Reactors by European Networks. Environ. Sci. Technol. 45, 7670-7677.

METI (Ministry of Economy, Trade and Industry), 2011a. http://www.meti.go.jp/press/2011/06/20110603019/20110603019.html (in Japanese, accessed on December 2, 2011).

METI, 2011b. http://www.meti.go.jp/press/20110316001/20110316001-2.pdf (in Japanese, accessed on December 2, 2011).

MEXT (Ministry of Education, Culture, Sports, Science and Technology), 2011a. Reading of environmental radioactivity level by prefecture. http://radioactivity.mext.go.jp/en/list/192/list-1.html (accessed on May 4, 2012).

MEXT, 2011b. Readings of dust sampling.

http://radioactivity.mext.go.jp/en/list/200/list-1.html (accessed on May 4, 2012).

MEXT, 2011c. Reading of radioactivity level in fallout by prefecture.

http://radioactivity.mext.go.jp/en/list/194/list-1.html (accessed on May 4, 2012).

MEXT, 2011d. MEXT and DOE Airborne Monitoring.

http://radioactivity.mext.go.jp/en/list/203/list-1.html (accessed on May 4, 2012).

MEXT, 2011e. Distribution map of radiation dose around Fukushima Dai-ichi&Dai-Ni NPP.

http://radioactivity.mext.go.jp/en/list/255/list-1.html (accessed on May 4, 2012).

MEXT, 2011f. Reading of radioactivity level in drinking water by prefecture.

http://radioactivity.mext.go.jp/en/list/193/list-1.html (accessed on May 4, 2012).

MHLW (Ministry of Health, Labour and Welfare), 2011.

http://www.mhlw.go.jp/english/topics/2011eq/dl/20110930_20110319.pdf (accessed on May 4,

2012).

Miyagi Prefecture, 2011. http://www.pref.miyagi.jp/gentai/Press/PressH230315-3(sokutei).html (in Japanese, accessed on December 2, 2011).

TEPCO (Tokyo Electric Power Company), 2011a. Additional monitoring data at Fukushima Daiichi Nuclear Power Station.

http://www.tepco.co.jp/en/press/corp-com/release/11052811-e.html (accessed on December 2, 2011).

TEPCO, 2011b. http://www.tepco.co.jp/en/press/corp-com/release/index1103-e.html (accessed on December 2, 2011).

Terada, H., Furuno, A., Chino, M., 2004. Improvement of Worldwide Version of System for Prediction of Environmental Emergency Dose Information (WSPEEDI), (I) New combination of models, atmospheric dynamic model MM5 and particle random walk model GEARN-new. J. Nucl. Sci. Technol. 41, 632-640.

Terada, H. and Chino, M., 2005. Improvement of Worldwide Version of System for Prediction of Environmental Emergency Dose Information (WSPEEDI), (II) Evaluation of numerical models by ^{137}Cs deposition due to the Chernobyl nuclear accident. J. Nucl. Sci. Technol. 42, 651-660.

Terada, H. and Chino, M., 2008. Development of an atmospheric dispersion model for accidental discharge of radionuclides with the function of simultaneous prediction for multiple domains and its evaluation by application to the Chernobyl nuclear accident. J. Nucl. Sci. Technol. 45, 920-931.

Terada, H., Nagai H., Furuno, A., Kakefuda T., Harayama T., Chno M., 2008. Development of Worldwide version of system for prediction of environmental emergency dose information: WSPEEDI 2nd version. Transactions of the Atomic Energy Society of Japan. 7, 257-267 (in Japanese with English abstract).

Tochigi Prefecture, 2011. http://www.pref.tochigi.lg.jp/kinkyu/documents/20110312-18.pdf (in Japanese, accessed on December 2, 2011).

Tohoku Electric Power, 2011.

http://www.tohoku-epco.co.jp/news/atom/topics/1183332_1984.html (in Japanese, accessed on December 2, 2011).

Tokyo Metropolitan Government, 2011.

http://www.sangyo-rodo.metro.tokyo.jp/whats-new/measurement-kako.html (in Japanese, accessed on December 2, 2011).

SUPPLEMENTARY MOVIE CAPTIONS

Movie A1

Spatial distribution of cumulative surface ^{137}Cs deposition (Bq m^{-2}) (shaded areas) and surface concentrations of ^{137}Cs (Bq m^{-3}) (blue contour lines) calculated using the refined source term from 5 JST on March 12 to 0 JST on May 1, 2011.

TABLE CAPTIONS

Table 1.

Simulation conditions for atmospheric dynamic model (MM5) and atmospheric dispersion model (GEARN).

Table 2.

Release period, release duration, ^{131}I release rate, $^{131}I/^{137}Cs$ radioactivity ratio, release height, and references in which each source term was estimated or refined, for the period between 5 JST on March 12 and 0 JST on May 1, 2011. The values in parentheses are from Chino et al. (2011).

Table 3.

Statistics of daily surface deposition of ^{131}I and ^{137}Cs calculated from data points, for which both measured and calculated values were larger than 0.1 Bq m^{-2} between March 18 and April 30, 2011. The values of FA2, FA5, and FA10 denote the percentage of calculations within factors of 2, 5, and 10 of the measurements, respectively.

Table 1

Simulation period for GEARN	5 JST on March 12 to 0 JST on May 1, 2011
Simulation area	690 km × 960 km in eastern Japan (see Fig. 1)
Horizontal grid cell	230 × 320
Spatial resolutions	3 km
Vertical levels of MM5	31 sigma levels from surface to 100 hPa
Vertical levels of GEARN	29 levels from surface (with a bottom layer of 20-m thickness) to 10 km
Time step	9 s for MM5 and 12 s for GEARN
Boundary and initial conditions	Grid Point Value (GPV) of Meso-scale model (MSM) (0.1° × 0.125° for pressure level, 0.05° × 0.0625° for the surface layer) by the Japan meteorological agency
3D/surface analysis nudging[a]	Utilized at 1-h intervals with wind data from MSM objectively analyzed by observation data at FNPP1 (surface), FNPP2 (120 m), and surface weather stations by the Japan meteorological agency
Observation nudging[a]	Utilized at 1-h intervals with wind data at FNPP1 (surface) and FNPP2 (120 m)
Other parameters and settings	Same as Katata et al. (2012b)

[a] Wind data at FNPP1 and FNPP2 were provided from METI (2011b).

Table 2

No.	Release period (month/day time JST)	Release duration (h)	Release rate of ^{131}I (Bq h^{-1})	$^{131}I/^{137}Cs$	Release height (m)	References
1	3/12 05:00–3/12 09:30	4.5	3.7×10^{13}	10	20	Katata et al. (2012b)
2	3/12 09:30–3/12 15:30	6	1.7×10^{13}	10	120	Katata et al. (2012b)
3	3/12 15:30–3/12 16:00	0.5	3.0×10^{15}	10	Volume source[a]	Katata et al. (2012b)
4	3/12 16:00–3/13 23:00	31	8.4×10^{13}	10	120	Katata et al. (2012b)
5	3/13 23:00–3/14 11:00	12	3.6×10^{13}	10	120	Katata et al. (2012b)
6	3/14 11:00–3/14 11:30	0.5	3.0×10^{15}	10	Volume source[a]	Assumed same as No.
7	3/14 11:30–3/14 21:30	10	2.3×10^{13}	10	20	Chino et al. (2011)
8	3/14 21:30–3/15 00:00	2.5	1.3×10^{15}	10	120	Katata et al. (2012b)
9	3/15 00:00–3/15 07:00	7	3.5×10^{14}	8.8	120	Chino et al. (2011)
10	3/15 07:00–3/15 10:00	3	3.0×10^{15}	10	20	Katata et al. (2012a)
11	3/15 10:00–3/15 13:00	3	8.0×10^{13}	10	20	Katata et al. (2012a)
12	3/15 13:00–3/15 17:00	4	4.0×10^{15}	10	20	Katata et al. (2012a)
13	3/15 17:00–3/17 06:00	37	2.1×10^{14}	70	20	Chino et al. (2011)
14	3/17 06:00–3/19 15:00	57	4.1×10^{14}	41	20	Chino et al. (2011)
15	3/19 15:00–3/21 03:00	36	3.8×10^{14}	11	20	Chino et al. (2011)
16[b]	3/21 03:00–3/21 21:00	18	1.4×10^{14}	10 (131)	20	This study
17	3/21 21:00–3/22 23:00	26	4.1×10^{14}	87	20	Chino et al. (2011)
18	3/22 23:00–3/24 00:00	25	7.1×10^{14}	80	20	Chino et al. (2011)
19	3/24 00:00–3/25 00:00	24	1.9×10^{14}	66	20	Chino et al. (2011)
20	3/25 00:00–3/26 11:00	35	5.6×10^{13}	45	20	Chino et al. (2011)
21	3/26 11:00–3/28 10:00	47	4.0×10^{12}	23	20	Chino et al. (2011)
22	3/28 10:00–3/29 21:00 (3/28 10:00–3/30 00:00)	35 (38)	7.5×10^{12}	1.6	20	Chino et al. (2011)
23[c]	3/29 21:00–3/30 11:00	14	1.5×10^{13}	1.7	20	This study
24	3/30 11:00–3/31 00:00 (3/30 00:00–3/31 00:00)	13 (24)	1.8×10^{14}	1.3	20	Chino et al. (2011)
25	3/31 00:00–3/31 22:00	22	2.4×10^{13}	5.3	20	Chino et al. (2011)
26	3/31 22:00–4/2 09:00	35	1.8×10^{12}	1.1	20	Chino et al. (2011)
27	4/2 09:00–4/4 09:00	48	1.8×10^{12}	3.1	20	Chino et al. (2011)
28	4/4 09:00–4/7 17:00 (4/4 09:00–4/6 00:00)	80	7.0×10^{11}	4.9	20	Chino et al. (2011)
29[d]	4/7 17:00–4/13 23:00	150	7.0×10^{11}	2.0	20	This study
30[d]	4/13 23:00–5/1 00:00	409	7.0×10^{11}	4.0	20	This study

[a] Volume sources with the sizes of (x, y, z) = (100, 100, 100 m) and (100, 100, 300 m) were assumed for hydrogen explosions at Unit 1 (No. 3) and 3 (No. 6), respectively.

[b] The $^{131}I/^{137}Cs$ radioactivity ratio was decided on the basis of dust sampling data at FNPP2 (TEPCO, 2011b), Tokai (Furuta,et al., 2011) and Setagaya (Tokyo Metropolitan Government, 2011).

[c] The ^{131}I release rate was estimated from the concentration of ^{131}I at FNPP2 by dust sampling from 9:27 to 9:35 on March 30 to be, 1490 Bq m^{-3} (TEPCO, 2011b), and that by calculation assuming unit release to be, 1.0×10^{-10} Bq m^{-3}. The release time of sampled air was estimated to be 8:00 on March 30.

[d] The $^{131}I/^{137}Cs$ radioactivity ratios were determined from the dust sampling data at Tokai (Furuta et al., 2011). Release times of the plumes for Nos. 29 and 30 were estimated at 0:00 on April 10 and 22:00 on April 17, respectively.

Table 3

Release rate used for calculations	Radionuclides	FA2 (%)	FA5 (%)	FA10 (%)	Correlation coefficients
Initial source term	^{131}I	23.5	51.6	67.3	0.76
	^{137}Cs	19.6	39.9	54.5	0.54
Refined source term	^{131}I	23.5	53.6	68.6	0.77
	^{137}Cs	23.8	46.3	62.6	0.74

FIGURE CAPTIONS

Figure 1.
The simulation area and locations of the environmental monitoring points used for verification and refinement of the source term. Triangles and circles on the map indicate the dust sampling points used in this study and all sampling points for daily surface deposition in the area, respectively. The names of the monitoring points for the dust sampling and for the daily surface deposition used for statistical analysis, and of prefectures where the monitoring points exist, are denoted in the table. Solid lines over land in Japan show boundaries of prefectures. The Kanto region consists of Ibaraki, Tochigi, Gunma, Saitama, Chiba, Tokyo, and Kanagawa Prefectures (Nos. 9-15).

Figure 2.
Temporal variation in the estimated release rates of ^{131}I and ^{137}Cs (a) from 5 JST on March 12 to 0 JST on April 6 and (b) from 0 JST on April 6 to 0 JST on May 1, 2011. Solid and dashed lines show release rates of ^{131}I and ^{137}Cs, respectively. Bold (red) and thin (black) lines represent the refined source term in this study and the initial source term, respectively. The latter was estimated by Chino et al. (2011) and Katata et al. (2012a, 2012b).

Figure 3.
Scatter diagrams of the daily surface deposition of ^{131}I and ^{137}Cs (Bq m^{-2}) comparing measurements and calculations using the (a) initial and (b) refined source terms. Dots (black) and crosses (blue) indicate the data points up to April 5 and after April 6, 2011, respectively. Solid lines show 1:1 lines, and the areas between two dashed lines indicate the bands within a factor of 10. Dates and numbers of the sampling points in Fig. 1 referred to in the text are indicated in the figure.

Figure 4.
Bland-Altman plots for differences in logarithm of the daily surface deposition of ^{131}I and ^{137}Cs between measurements and calculations (subtraction of measurements from calculations) using the (a) initial and (b) refined source terms. Solid lines with values on the right edges denote the mean values of the differences (MD). Two dashed lines with values on the right edges over and under the MD lines indicate MD+2SD and MD-2SD, respectively (SD : standard deviations of the differences).

Figure 5.
Comparison of the daily surface deposition of ^{137}Cs (Bq m^{-2}) from calculations using the initial source term (colored shades) with the corresponding measurements (colored circles and values) in the periods (a) from 9 JST on March 22 to 9 JST on March 23 and (b) from 9 JST on March 30 to 9 JST on March 31, 2011. Observation results that were not detectable are shown as 0 in the figures.

Figure 6.

Comparisons of daily surface deposition of ^{137}Cs (Bq m^{-2}) from calculations using the refined source term (colored shades) with the corresponding measurements (colored circles and values). Observation results that were not detectable are shown as 0 in the figures.

Figure 7.

Comparison of calculated (colored shades) and measured (colored circles and values) daily precipitation (cm day^{-1}).

Figure 8.

Comparison of the cumulative surface ^{137}Cs deposition (Bq m^{-2}) from calculations using the refined source term (colored shades) with the corresponding measurements (colored circles and values). The left (a) shows the result accumulated from 5 JST on March 12 to 0 JST on April 1 and the right (b) from 5 JST on March 12 to 0 JST on May 1, 2011. Observation results that were not detectable are shown as 0 in the figures.

Figure 9.

The calculated results with the refined source term of (a) wet deposition (Bq m^{-2}), (b) dry deposition (Bq m^{-2}), and (c) the ratio of wet deposition to the total of ^{137}Cs in the areas where the total deposition accumulated from 5 JST on March 12 to 0 JST on May 1, 2011 was greater than 100 Bq m^{-2}.

Figure 1

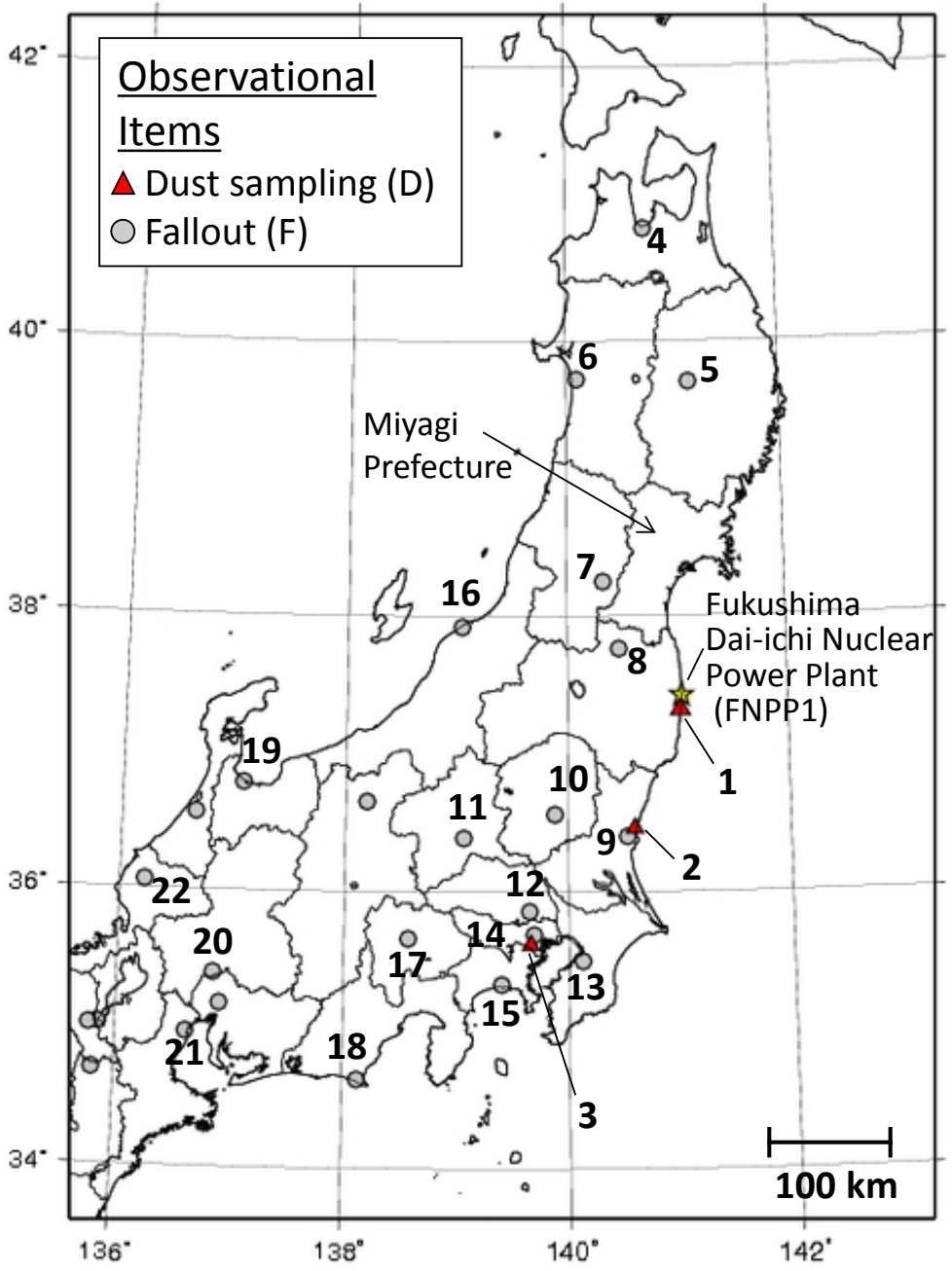

No.	Sampling sites	Prefectures	Items
1	Fukushima Dai-ni Nuclear Power Plant (FNPP2)	Fukushima	D
2	Tokai	Ibaraki	D
3	Setagaya	Tokyo	D
4	Aomori	Aomori	F
5	Morioka	Iwate	F
6	Akita	Akita	F
7	Yamagata	Yamagata	F
8	Fukushima	Fukushima	F
9	Hitachinaka	Ibaraki	F
10	Utsunomiya	Tochigi	F
11	Maebashi	Gunma	F
12	Saitama	Saitama	F
13	Ichihara	Chiba	F
14	Shinjuku	Tokyo	F
15	Chigasaki	Kanagawa	F
16	Niigata	Niigata	F
17	Kofu	Yamanashi	F
18	Omaezaki	Shizuoka	F
19	Imizu	Toyama	F
20	Kakamigahara	Gifu	F
21	Yokkaichi	Mie	F
22	Fukui	Fukui	F

Figure 2

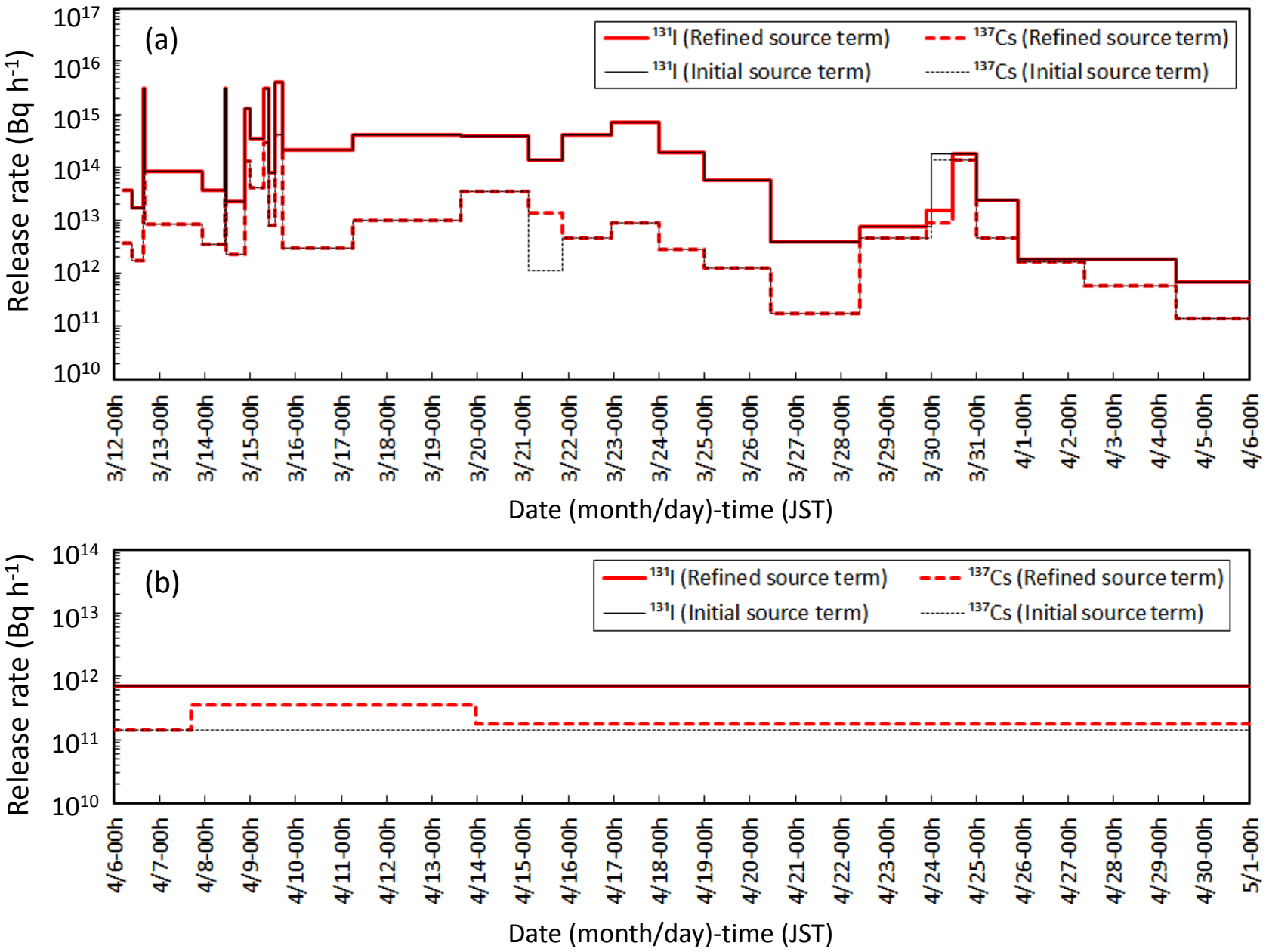
(a)
^{131}I (Refined source term)
^{137}Cs (Refined source term)
^{131}I (Initial source term)
^{137}Cs (Initial source term)
Release rate (Bq h^{-1})
10^{17}
10^{16}
10^{15}
10^{14}
10^{13}
10^{12}
10^{11}
10^{10}
3/12-00h
3/13-00h
3/14-00h
3/15-00h
3/16-00h
3/17-00h
3/18-00h
3/19-00h
3/20-00h
3/21-00h
3/22-00h
3/23-00h
3/24-00h
3/25-00h
3/26-00h
3/27-00h
3/28-00h
3/29-00h
3/30-00h
3/31-00h
4/1-00h
4/2-00h
4/3-00h
4/4-00h
4/5-00h
4/6-00h
Date (month/day)-time (JST)
(b)
^{131}I (Refined source term)
^{137}Cs (Refined source term)
^{131}I (Initial source term)
^{137}Cs (Initial source term)
Release rate (Bq h^{-1})
10^{14}
10^{13}
10^{12}
10^{11}
10^{10}
4/6-00h
4/7-00h
4/8-00h
4/9-00h
4/10-00h
4/11-00h
4/12-00h
4/13-00h
4/14-00h
4/15-00h
4/16-00h
4/17-00h
4/18-00h
4/19-00h
4/20-00h
4/21-00h
4/22-00h
4/23-00h
4/24-00h
4/25-00h
4/26-00h
4/27-00h
4/28-00h
4/29-00h
4/30-00h
5/1-00h
Date (month/day)-time (JST)

Figure 3

(a) Initial source term

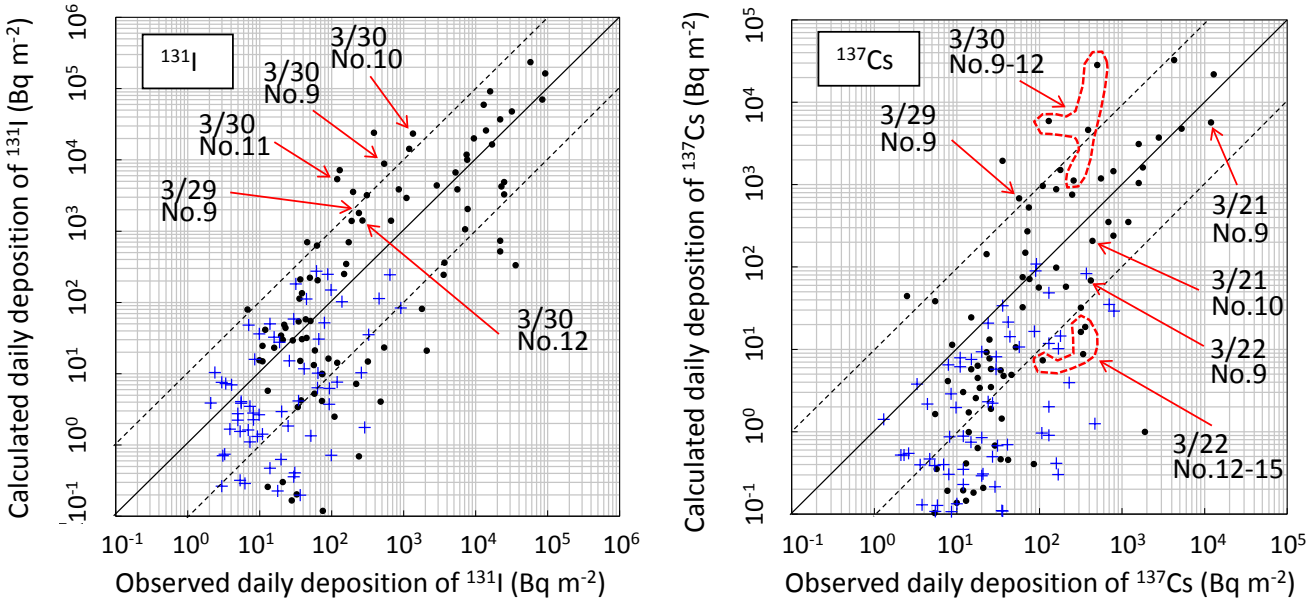

(b) Refined source term

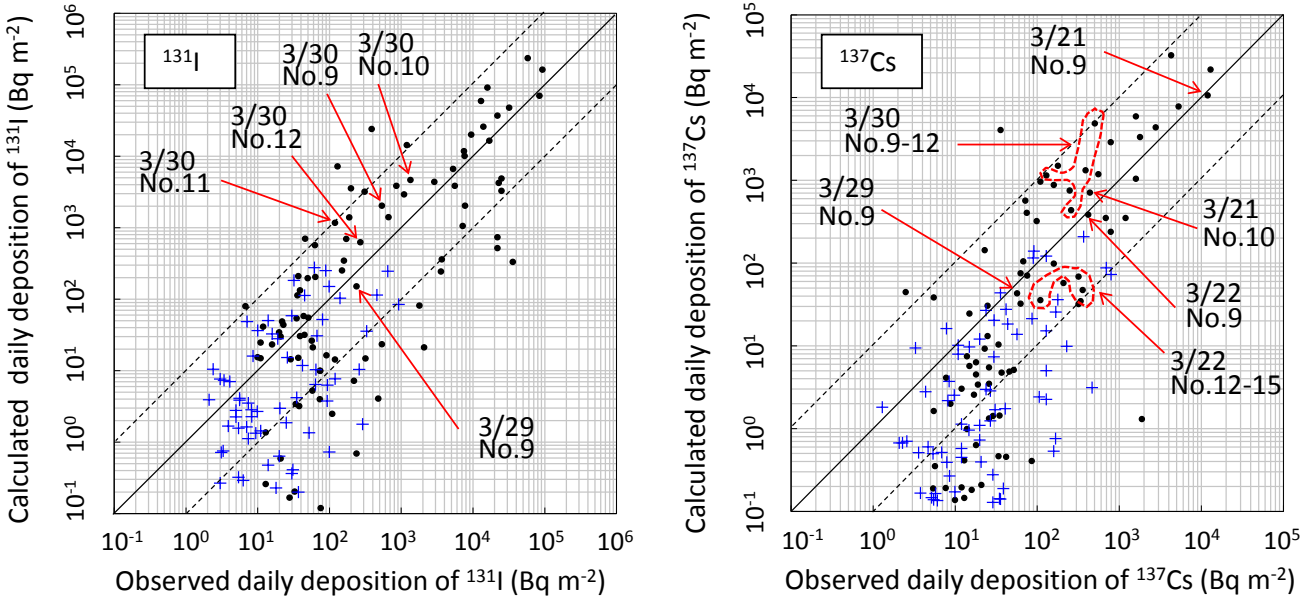

Figure 4

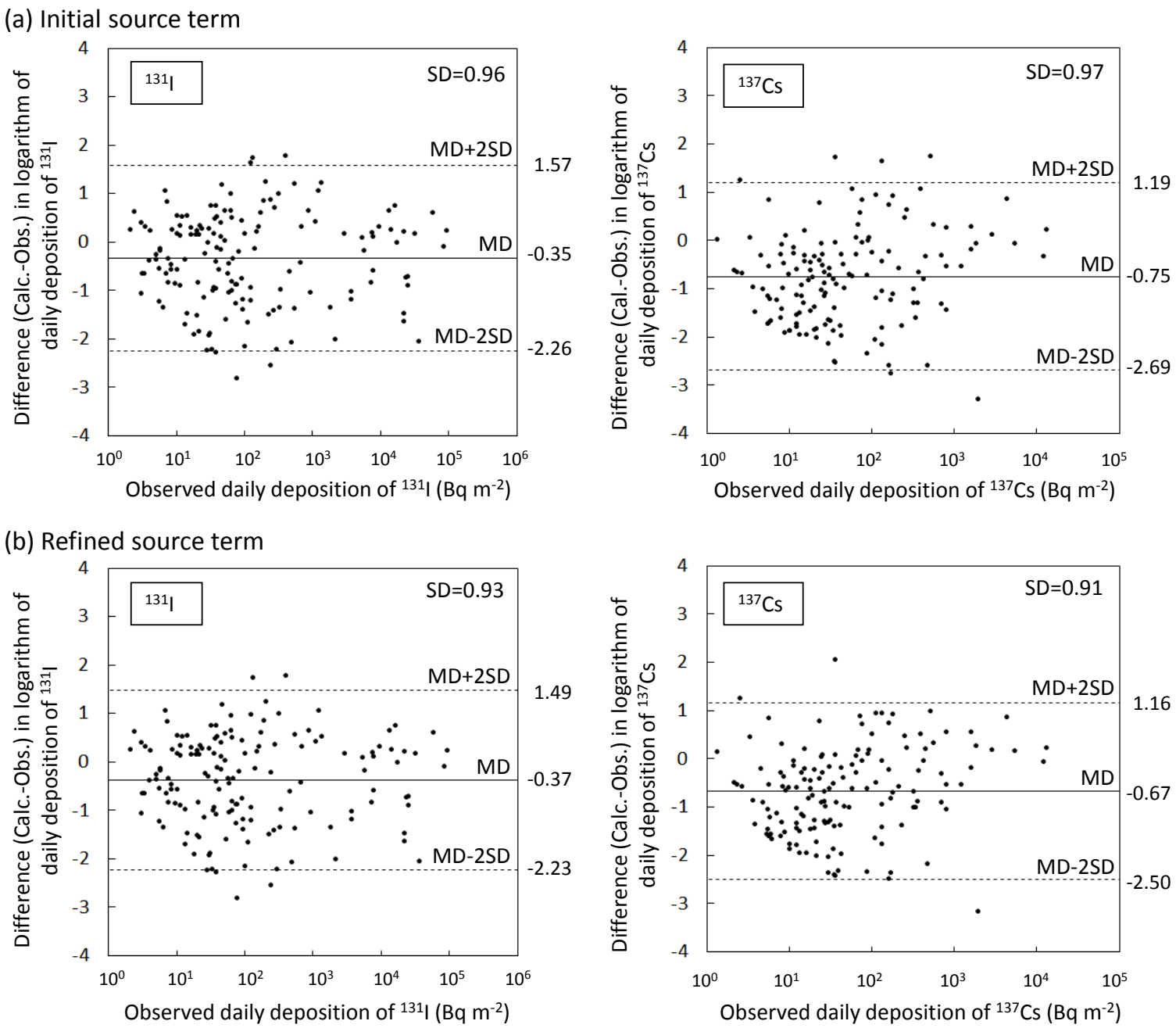
(a) Initial source term
131I
SD=0.96
MD+2SD
1.57
MD
-0.35
MD-2SD
-2.26
Difference (Calc.-Obs.) in logarithm of daily deposition of 131I
Observed daily deposition of 131I (Bq m-2)
137Cs
SD=0.97
MD+2SD
1.19
MD
-0.75
MD-2SD
-2.69
Difference (Cal.-Obs.) in logarithm of daily deposition of 137Cs
Observed daily deposition of 137Cs (Bq m-2)
(b) Refined source term
131I
SD=0.93
MD+2SD
1.49
MD
-0.37
MD-2SD
-2.23
Difference (Calc.-Obs.) in logarithm of daily deposition of 131I
Observed daily deposition of 131I (Bq m-2)
137Cs
SD=0.91
MD+2SD
1.16
MD
-0.67
MD-2SD
-2.50
Difference (Calc.-Obs.) in logarithm of daily deposition of 137Cs
Observed daily deposition of 137Cs (Bq m-2)

Figure 5

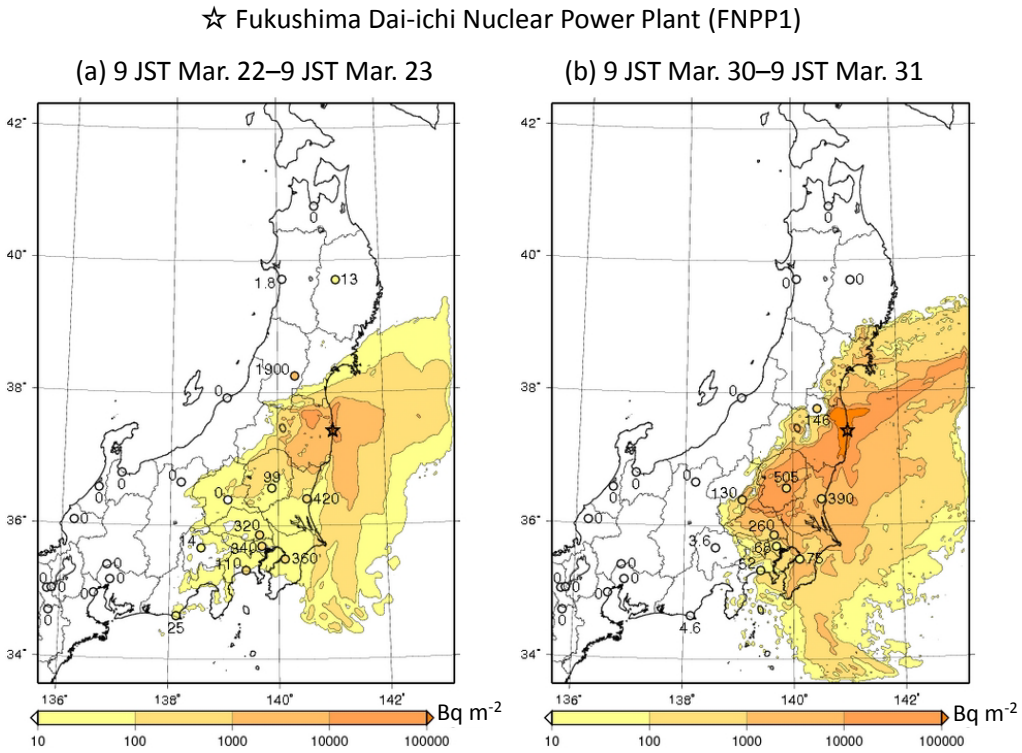
☆ Fukushima Dai-ichi Nuclear Power Plant (FNPP1)
(a) 9 JST Mar. 22–9 JST Mar. 23
(b) 9 JST Mar. 30–9 JST Mar. 31
42°
40°
38°
36°
34°
136°
138°
140°
142°
1.8
13
1900
99
420
320
14
340
110
360
25
146
505
130
390
260
3.6
68
52
75
4.6
Bq m-2
10
100
1000
10000
100000

Figure 6

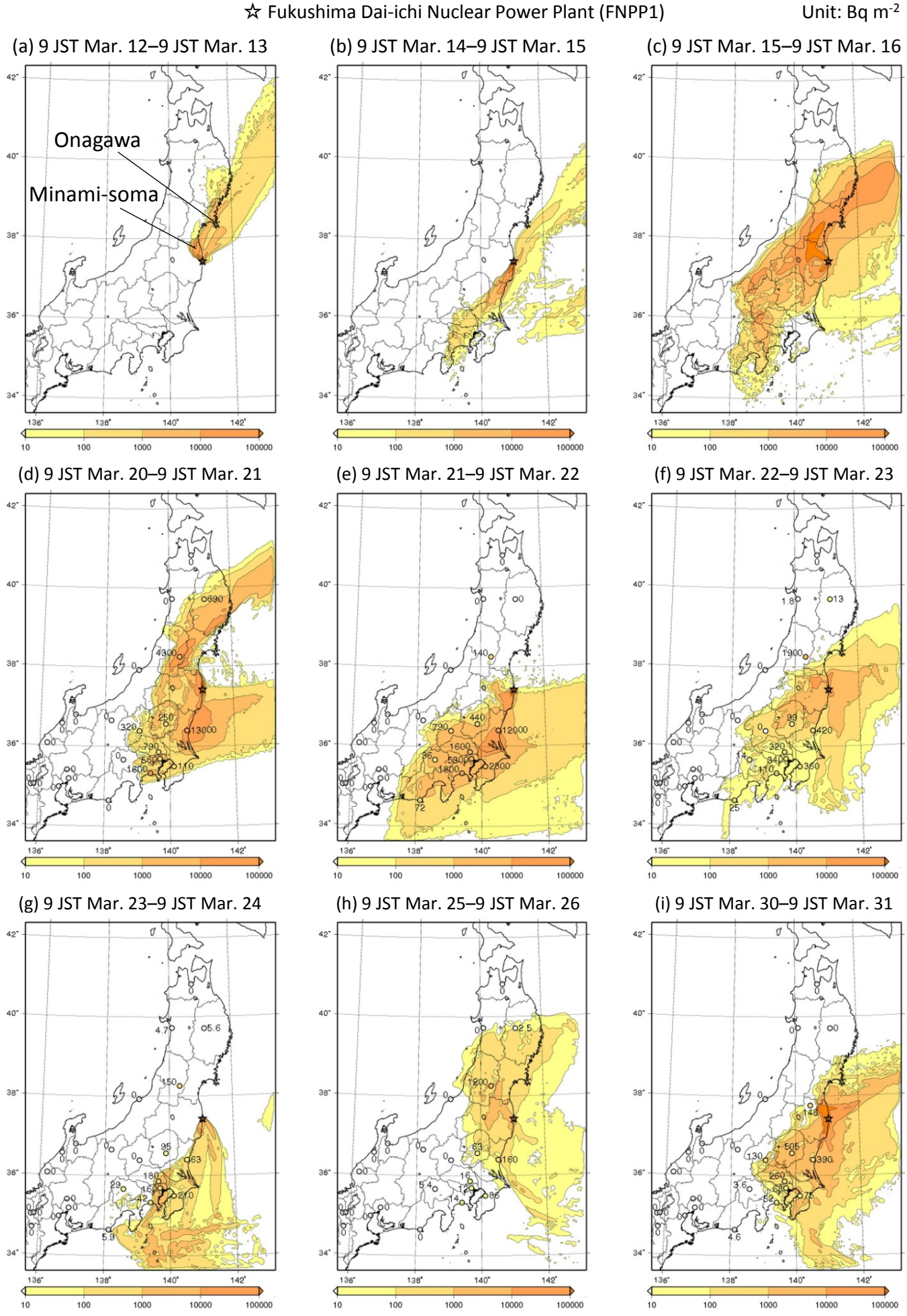
☆ Fukushima Dai-ichi Nuclear Power Plant (FNPP1)
Unit: Bq m-2
(a) 9 JST Mar. 12–9 JST Mar. 13
(b) 9 JST Mar. 14–9 JST Mar. 15
(c) 9 JST Mar. 15–9 JST Mar. 16
(d) 9 JST Mar. 20–9 JST Mar. 21
(e) 9 JST Mar. 21–9 JST Mar. 22
(f) 9 JST Mar. 22–9 JST Mar. 23
(g) 9 JST Mar. 23–9 JST Mar. 24
(h) 9 JST Mar. 25–9 JST Mar. 26
(i) 9 JST Mar. 30–9 JST Mar. 31
Onagawa
Minami-soma
10
100
1000
10000
100000

Figure 7

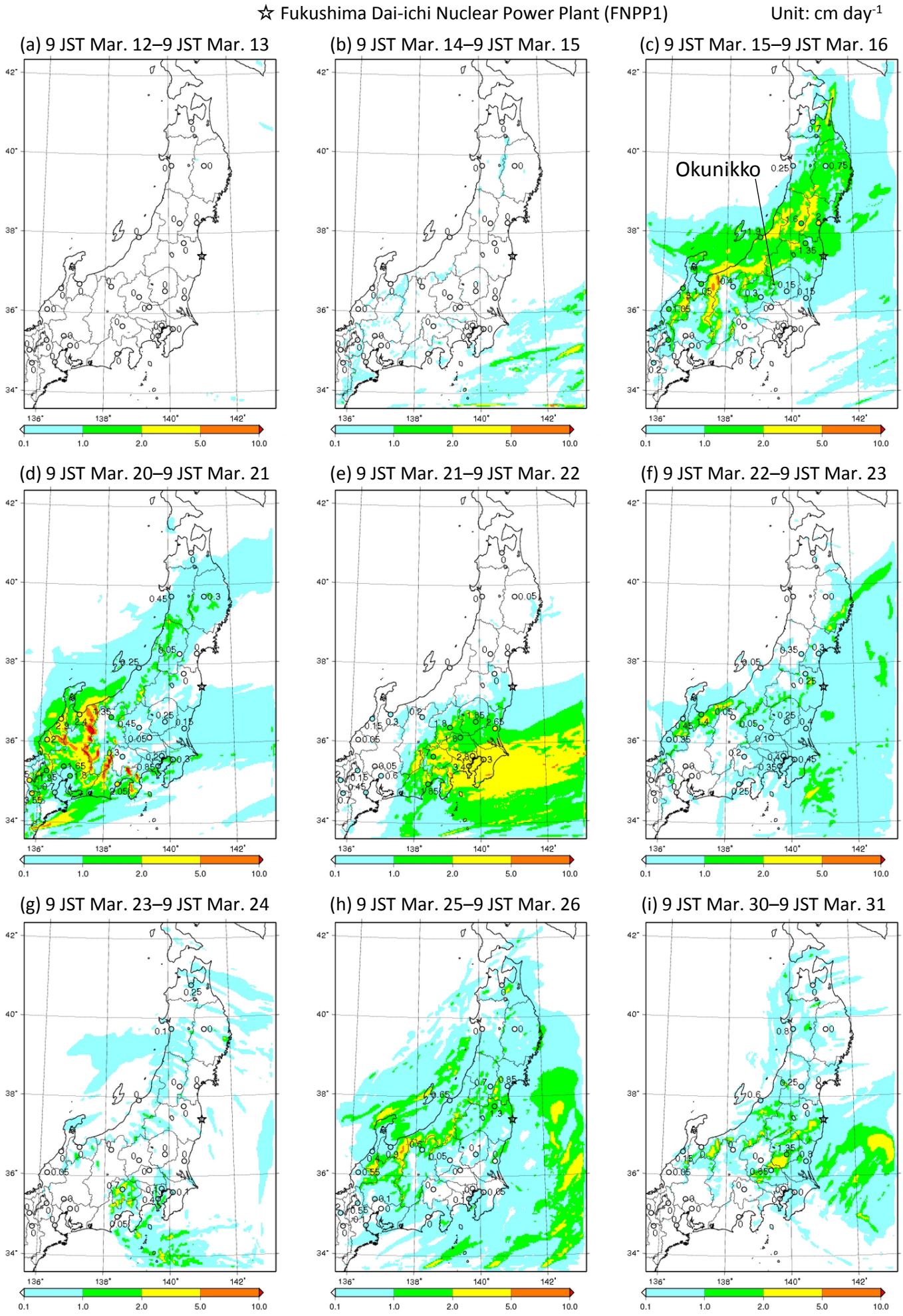
☆ Fukushima Dai-ichi Nuclear Power Plant (FNPP1)
Unit: cm day-1
(a) 9 JST Mar. 12–9 JST Mar. 13
(b) 9 JST Mar. 14–9 JST Mar. 15
(c) 9 JST Mar. 15–9 JST Mar. 16
Okunikko
(d) 9 JST Mar. 20–9 JST Mar. 21
(e) 9 JST Mar. 21–9 JST Mar. 22
(f) 9 JST Mar. 22–9 JST Mar. 23
(g) 9 JST Mar. 23–9 JST Mar. 24
(h) 9 JST Mar. 25–9 JST Mar. 26
(i) 9 JST Mar. 30–9 JST Mar. 31
136° 138° 140° 142°
42° 40° 38° 36° 34°
0.1 1.0 2.0 5.0 10.0

Figure 8

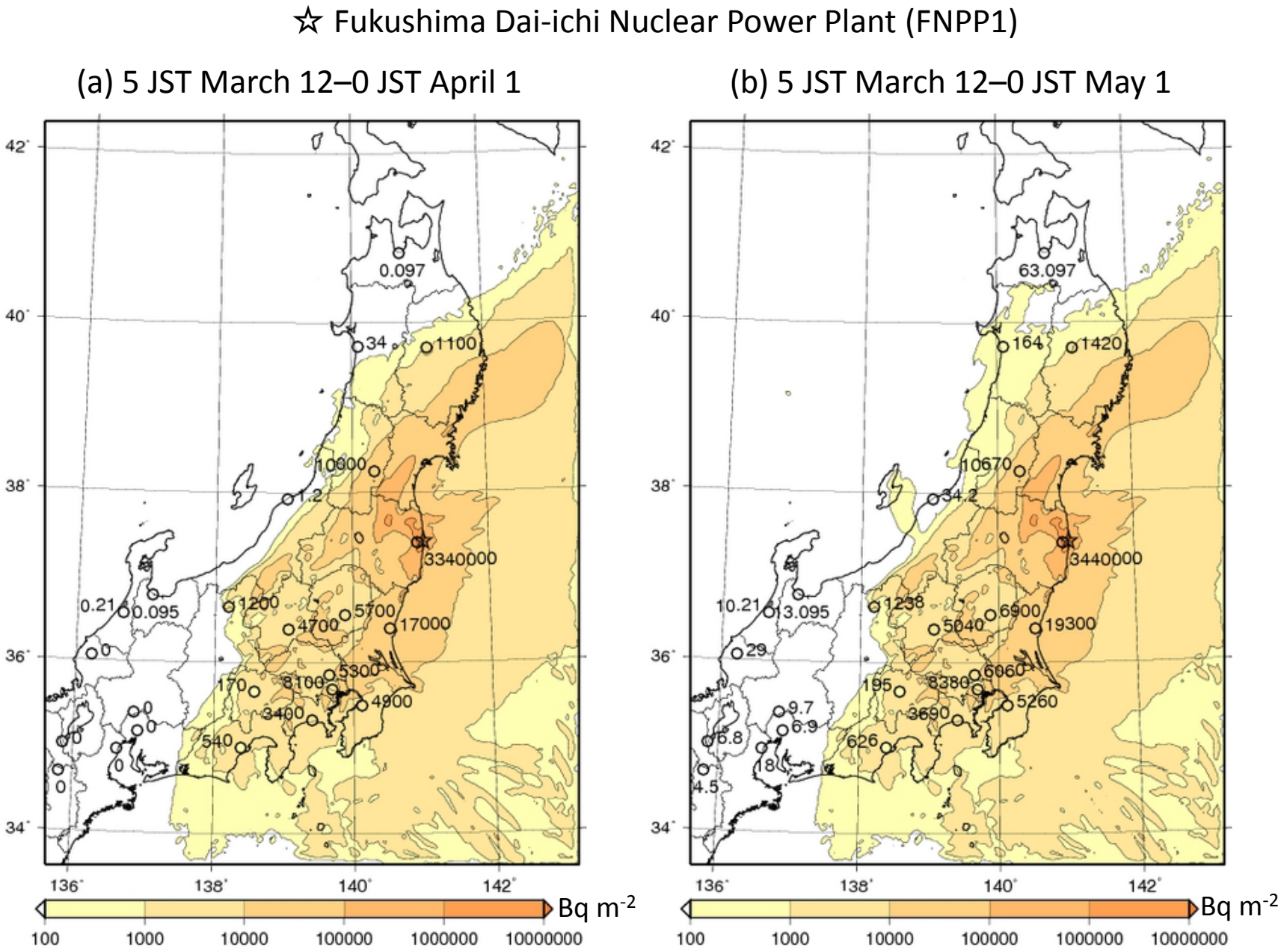
☆ Fukushima Dai-ichi Nuclear Power Plant (FNPP1)
(a) 5 JST March 12–0 JST April 1
(b) 5 JST March 12–0 JST May 1
42°
40°
38°
36°
34°
136°
138°
140°
142°
0.097
34
1100
10000
1.2
3340000
0.21
0.095
1200
4700
5700
17000
170
8100
5300
4900
3400
540
63.097
164
1420
10670
34.2
3440000
10.21
3.095
1238
5040
6900
19300
29
195
8380
6060
5260
3690
9.7
6.9
5.8
626
18
4.5
Bq m-2
100
1000
10000
100000
1000000
10000000

Figure 9

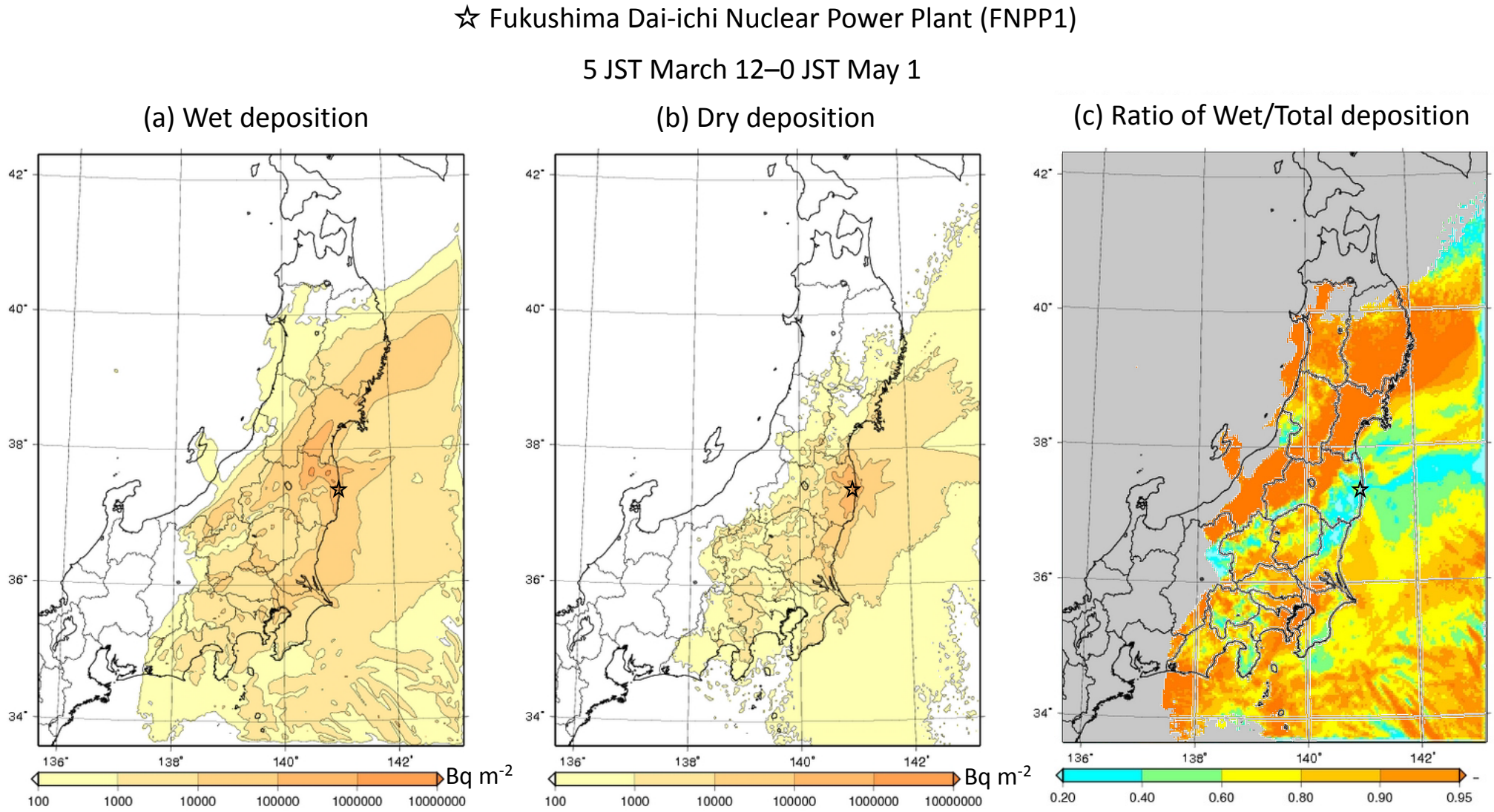
☆ Fukushima Dai-ichi Nuclear Power Plant (FNPP1)
5 JST March 12–0 JST May 1
(a) Wet deposition
(b) Dry deposition
(c) Ratio of Wet/Total deposition
42°
40°
38°
36°
34°
136°
138°
140°
142°
Bq m-2
100
1000
10000
100000
1000000
10000000
0.20
0.40
0.60
0.80
0.90
0.95
-